Online LiDAR-Camera Extrinsic Parameters Self-checking

Pengjin Wei*[a], Guohang Yan*[b], Yikang Li[b], Kun Fang[a], Jie Yang†[a], Wei Liu†[a]

***Abstract*— With the development of neural networks and the increasing popularity of automatic driving, the calibration of the LiDAR and the camera has attracted more and more attention. This calibration task is multi-modal, where the rich color and texture information captured by the camera and the accurate three-dimensional spatial information from the LiDAR is incredibly significant for downstream tasks. Current research interests mainly focus on obtaining accurate calibration results through information fusion. However, they seldom analyze whether the calibrated results are correct or not, which could be of significant importance in real-world applications. For example, in large-scale production, the LiDARs and the cameras of each smart car have to get well-calibrated as the car leaves the production line, while in the rest of the car life period, the poses of the LiDARs and cameras should also get continually supervised to ensure the security. To this end, this paper proposes a self-checking algorithm to judge whether the extrinsic parameters are well-calibrated by introducing a binary classification network based on the fused information from the camera and the LiDAR. Moreover, since there is no such dataset for the task in this work, we further generate a new dataset branch from the KITTI dataset tailored for the task. Our experiments on the proposed dataset branch demonstrate the performance of our method. To the best of our knowledge, this is the first work to address the significance of continually checking the calibrated extrinsic parameters for autonomous driving. The code is open-sourced on the Github website at `https://github.com/OpenCalib/LiDAR2camera_self-check`.**

I. INTRODUCTION

LiDAR is a kind of sensor that can obtain three-dimensional spatial coordinates. Compared with the camera, LiDAR can obtain accurate spatial information but less color and texture information than the camera. Therefore, in the automatic driving scenario, it is necessary to obtain a kind of data that combines the advantages of the two sensors, which can provide much more information for the downstream sensing tasks.

In practical applications, it is quite useful to judge whether the calibration result is accurate or not. Especially in the automatic driving scenario, the calibration performance should be analyzed and checked when the vehicle is manufactured. Production efficiency will be significantly improved if this process can be done automatically. Meanwhile, during the operation of the vehicle, all the sensors of the vehicle need to remain in the normal working state all the times. It requires tools to detect the sensor state so that in case of sensor offset or jitter, the vehicle can be braked immediately, and emergency measures can be taken. Timely detection and treatment can protect the safety of passengers.

Many existing works [27], [36], [37] focus more on improving the calibration accuracy, and no work has focused on judging the calibration results. However, detecting the accuracy of calibration parameters in real time is crucial to ensure the safe and stable operation of autonomous driving. Therefore, we adopt the powerful feature extraction and classification capabilities of deep learning to automatically detect the accuracy of calibration parameters in real time.

Therefore, we study this problem and propose a LiDAR-camera extrinsic parameters self-checking algorithm. Firstly, a 2D-3D problem is converted into a 2D-2D problem by projecting the point cloud onto the 2D space. The configuration of the sensor is shown in Fig 1. The depth image from the projection and the RGB image from the camera are fed into the feature extraction network to generate multi-scale features. The features of the RGB image and the depth image are fused and put into a classification network to check the calibration state. More importantly, to ensure that classification network could correctly check the calibration results, corresponding positive and negative samples are created to train the network via adding random perturbations on the groundtruth. The resulting dataset will be released.

The proposed method could achieve fascinating self-checking accuracy on the calibrated results with strong robustness and high processing speed, which we believe will benefit the autonomous driving community a lot. The contributions of this work are as follows:

1) To the best of our knowledge, we are the first to address the significance of judging the accuracy of the calibrated extrinsic parameters in autonomous driving, and we further propose a self-checking algorithm.
2) The proposed self-checking algorithm adopts a binary classification network on the fused information to judge the calibration results. Moreover, a strategy is devised to create sufficient and reasonable positive and negative samples so that the trained classification network can check the correctness of the calibrated results.
3) The proposed method shows promising performance on the data generated from the KITTI dataset; meanwhile, the code has been open-sourced to benefit the community.

The rest of this paper is organized as follows: section II briefly presents related works about LiDAR and camera extrinsic parameters calibration. Section III details each

* Equally contribution.
† Corresponding author.
[a] P. Wei, K. Fang, W. Liu, J. Yang are with the Institute of Image Processing and Pattern Recognition; Department of Automation; Shanghai Jiao Tong University, China. {pengjinwei, fanghenshao, weiliucv, jieyang}@sjtu.edu.cn
[b] G. Yan, Y. Li are with the Autonomous Driving Group, Shanghai AI Laboratory, China. {yanguohang, liyikang}@pjlab.org.cn

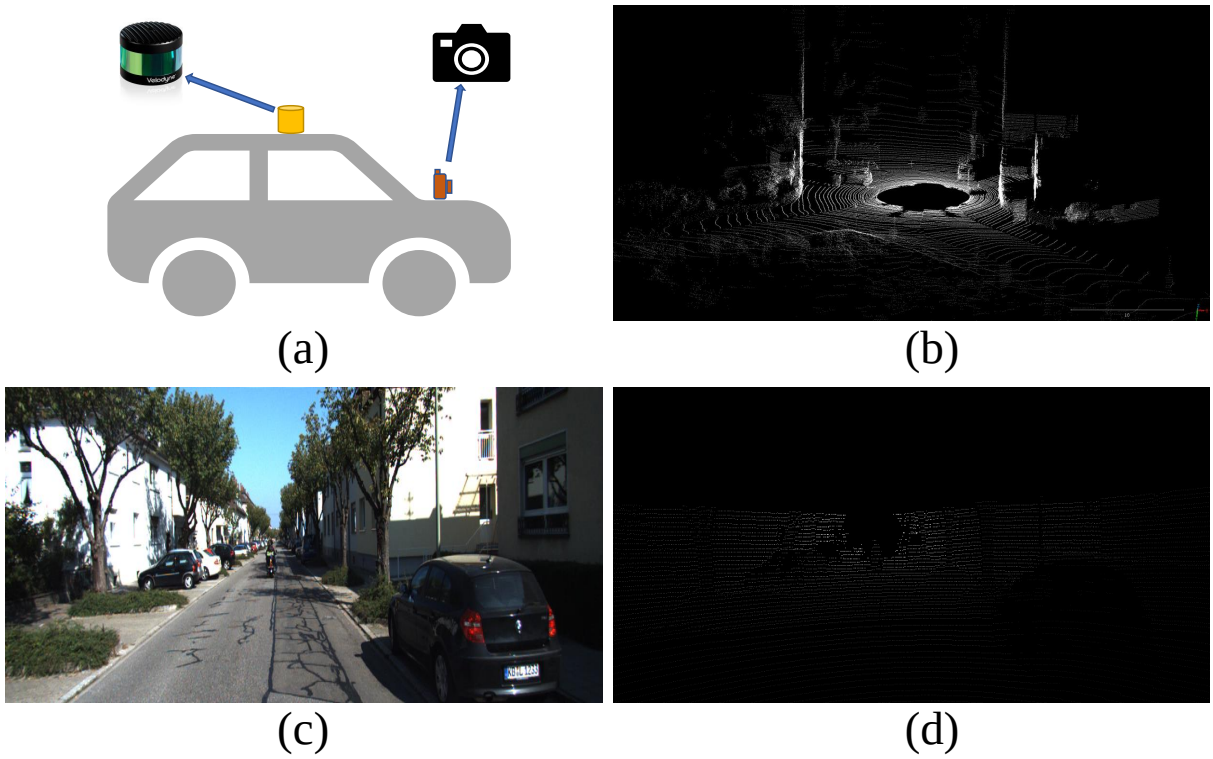

Fig. 1: (a) The configuration of the LiDAR and camera used in this work. (b) The raw point cloud of the LiDAR. (c) The RGB image of the camera. (d) The depth image of the point cloud projection.

component of our method, including data preparation, feature extraction, feature fusion and binary classification. Our method is evaluated on the public dataset in section IV. We conclude this paper in section V.

II. RELATED WORK

There are few researchers studying online self-checking of calibration parameters. However, calibration parameter self-checking and calibration are mutually related, and there are a lot of research and mature algorithms for LiDAR-camera calibration. According to different information extraction methods, the online LiDAR-camera calibration can be divided into three methods: edge registration [13], mutual information [14], and segmentation [15], [17]. There are more methods based on calibration boards, for example, the recent work proposed in [18] performs LiDAR-camera joint calibration using a special calibration board.

2D-related works and experience benefit the 2D-3D task; 2D-3D registration can sometimes be converted into a 2D-2D problem. This is because they have a similar process: feature extraction, feature matching, parameter estimation and image re-sampling. In traditional methods, feature extraction is to extract salient features of images, such as points, lines, edges, contours, etc. The similar extracted features mean that images have similar elements. Common feature detection methods include scale-invariant feature transform (SIFT) [34] and speeded up robust features (SURF) [35], and so on. Feature matching establishes the corresponding relationship between the features detected by the reference images. In order to establish an accurate correspondence, different feature descriptors and similarity measures need to be used. It is worth mentioning that the feature descriptor should be robust against the rotation, translation, scaling and illumination of the image. Parameter estimation is to select a suitable transformation model and estimate the transformation parameters of the model according to the corresponding relationship between features. The final image re-sampling step is to re-sample and align the images using the estimated transformation parameters.

For 3D point cloud registration, classical methods include iterative closest point (ICP) [20], [21], normal-distributions transform (NDT) [22], and variations of ICP such as normal iterative closest point (NICP) [19]. Recent studies have also focused on calibrating surround-view LiDARs using 3D point cloud registration. For example, Wei et al. [26] propose a method for calibrating surround-view LiDARs in road scenes.

In recent years, deep learning networks have shown effectiveness in dealing with 2D and 3D computer vision tasks such as localization, object detection, and segmentation. A few works also apply deep learning to sensor calibration tasks, especially applying to the camera and LiDAR calibration problems. There are some methods [23]–[25] for 3D registration using deep learning. For LiDAR-camera calibration, Schneider et al. [2] propose the first deep convolution neural network RegNet for LiDAR-camera calibration. Their method infers extrinsic parameters directly by regressing to calibration parameters based on a supervised network. To fur-

ther involve spatial information and eliminate the influence of intrinsic parameters, Iyer et al. [3] propose a geometrically supervised network CalibNet for LiDAR-camera calibration, which reduces the dense photometric error and dense point cloud distance error. RGGNet [4] considers Riemannian geometry and utilizes a deep generative model to learn an implicit tolerance model for LiDAR-camera calibration. In comparison, there are much fewer learning-based approaches for intrinsic calibration problems. DeepCalib [11] proposes a CNN-based approach for intrinsic calibration of wide FOV cameras with an automatically generated large-scale intrinsic dataset. Because of less intuitive spatial relations in camera intrinsic calibration problems and high-precision requirements, learning-based methods have shown fewer advantages. Aside from end-to-end deep learning network for sensor calibration, some work on relevant vision tasks can be adapted as key partitions of the calibration process, such as vanishing point detection [5], car heading prediction [9] and camera pose estimation [6]–[8], [10], [12]. The learning-based approaches utilize the advantages of deep learning for more efficient spatial feature extraction and matching. The accuracy of many tasks classified by models in the visual field has surpassed that of humans. Therefore, inspired by [27]–[29], we propose to use the ability of deep learning to automatically detect the accuracy of calibration parameters in real time, which can further ensure the safety and stability of autonomous driving.

III. METHODOLOGY

The LiDAR is a 3D sensor, and the camera is a 2D sensor. We set the points cloud as $P_i = [X_i, Y_i, Z_i] \in R^3$, and set the 2D pixel coordinate as $p_i = [u_i, v_i] \in R^2$. The data structure of these two sensor is quite different. The first problem is to choose the appropriate data form, and there are two methods to select. The first one is to utilize the 3D reconstruction technology to transform the 2D RGB picture and generate the new data with geometric information. The other one is to project the point cloud onto a 2D plane. Compared with complex 3D reconstruction, projection is much more reliable and mature. The process of applying extrinsic and intrinsic parameters to the point cloud is shown in equation (1).

$$\begin{aligned}\left[\begin{array}{c|c} p_i & \mathbf{1} \end{array}\right]' &= \mathbf{K}\cdot\mathbf{T}\cdot\left[\begin{array}{c|c} P_i & \mathbf{1} \end{array}\right]' \\ &= \begin{bmatrix} 1 & 0 & x_0 \\ 0 & 1 & y_0 \\ 0 & 0 & 1 \end{bmatrix}\begin{bmatrix} 1 & s/f_y & 0 \\ 0 & 1 & 0 \\ 0 & 0 & 1 \end{bmatrix}\begin{bmatrix} f_x & 0 & 0 \\ 0 & f_y & 0 \\ 0 & 0 & 1 \end{bmatrix} \\ &\quad \left[\begin{array}{c|c} \mathbf{I} & \mathbf{t} \end{array}\right]\begin{bmatrix} \mathbf{R} & \mathbf{0} \\ \mathbf{0} & \mathbf{1} \end{bmatrix}\left[\begin{array}{c|c} P_i & \mathbf{1} \end{array}\right]', \end{aligned} \tag{1}$$

where $\mathbf{K}, \mathbf{T}$ represent the intrinsic and extrinsic parameters respectively, x_0, y_0 represent the principal point offset, s represents the axis skew, and f_x, f_y represent the focal length. $\mathbf{I}$ and $\mathbf{R}$ represent the extrinsic translation vector and rotation matrix, respectively.

Therefore, in our method, we first assume an extrinsic parameter transformation matrix $\boldsymbol{T}$ and transform the point cloud by $\boldsymbol{T}$. The point cloud is then projected onto the 2D plane using the intrinsic parameters $\boldsymbol{K}$, which results in the depth image. Our model can determine whether the depth map and RGB map are aligned. It returns a positive label if they are aligned and a negative label otherwise. In this section, we first describe a KITTI-based calibration judgment dataset. Then, we describe our proposed method, including the network architecture, loss functions, and training details. The pipline of our proposed method is shown in Fig. 2.

A. KITTI-based calibration judgment dataset

Currently, there is no dataset directly used to judge whether the calibration is accurate or not. However, the dataset can be obtained by modifying the existing dataset with accurate calibration parameters. KITTI [30] is a widely used computer vision dataset captured using an array of sensors mounted on top of the vehicle. Sensors for recording include two front-facing cameras and a Velodyne 3D-LiDAR. Several benchmarks have been published for various applications such as object detection [40], [41], depth estimation [38], [39] and semantic segmentation [31]. There is no benchmark for self-checking of calibration parameters. However, we can build it with some random perturbation using the precise calibration parameters provided by KITTI at no extra cost.

We introduce the KITTI calibration judgment dataset, a new addition to the KITTI raw dataset [30] with calibration parameter judgment annotations for all sequences. There are only two categories in the calibration judgment dataset. The point clouds with the accurate rigid transformation matrix are positive samples, and those with the incorrect rigid transformation matrix are negative. Considering the sensor error and the environment noise, we allow a small shift in the positive samples. Another detail that should be noticed is that extrinsic parameter calibration is a problem with 6 degrees of freedom, including $Roll, Pitch, Yaw, x, y, z$. Each one has two statuses: correct and incorrect. So every rigid transformation could have 2^6 conditions, and only one of these conditions is correct, and the rest are incorrect. As a binary classification problem, in both training data or test data, we generate equal positive and negative samples with correct rigid transformation $T_{correct}$ and incorrect rigid transformation $T_{incorrect}$. Both the positive samples and the negative samples are generated through equation (2) with $T_{disturbance}$ equals to $T_{correct}$ for the positive samples and $T_{incorrect}$ for the negative samples.

$$\left[\begin{array}{c|c} p_i & \mathbf{1} \end{array}\right]' = \mathbf{K}\cdot\mathbf{T}_{\mathbf{disturbance}}\cdot\mathbf{T}_{\mathbf{initial}}\cdot\left[\begin{array}{c|c} P_i & \mathbf{1} \end{array}\right]'. \tag{2}$$

B. Framework

Our LiDAR-camera extrinsic parameters self-checking network includes a feature extraction module, feature fusion module and binary classification module, as shown in Fig. 2. Given the RGB and depth images, we use two symmetric stream networks to extract high-level features. For the RGB stream, we adopt a pre-trained ResNet-18 network [42]. Meanwhile, we also use a ResNet-18 network and replace the origin activation function with Leaky RELU [43]. It should

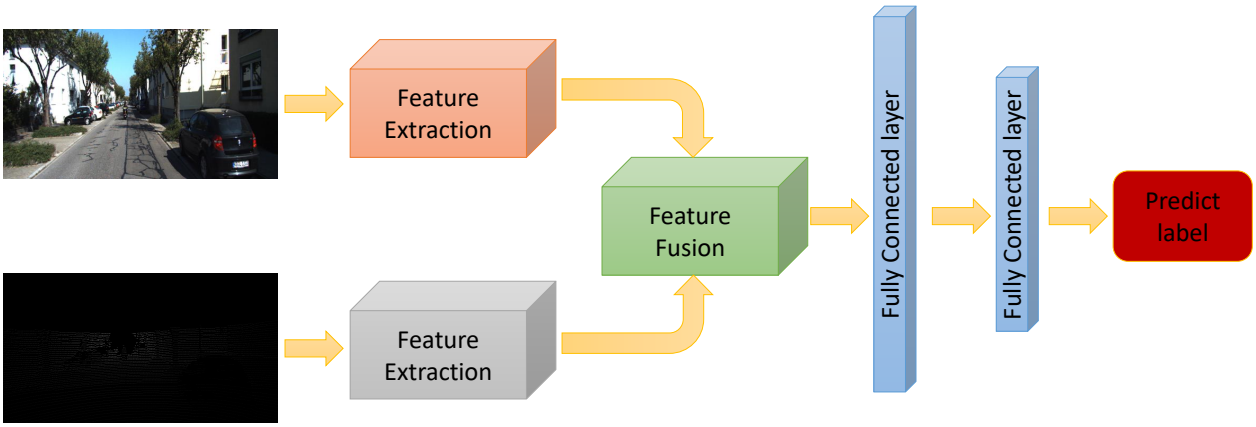

Fig. 2: The structure of our LiDAR-camera calibration self-checking network.

be noted that we omit the fully connected layers in both two ResNet-18 networks. Inspired by LCCNet [27] and PWC-Net [32], we use the inner product to fuse the two-modal features. The output of two feature extraction networks has high-dimension features and small size. During the feature fusing, only adjacent pixels features are considered to fuse. This operation significantly reduces the computation complexity and improves the expression ability of the fused feature map. After that, the fused feature map is fed into a convolutional network, and a larger-size feature map is generated, which is the same as the input RGB image. This operation generates dense features, and it can be regarded as feature upsampling. Our goal is to check the status of the sensor calibration, and it only requires one label. We thus add two fully connected layers after the feature fusion module to predict the result. The fully connected layer can link each pixel of the feature map and converge all the information to generate the final judgment. Thus, every pixel can influence the result, and such a mechanism is appropriate for a highly accurate and robust calibration status check. Since LiDAR-Camera extrinsic self-check is a classification task, we thus use the cross entropy to measure the ability of the network.

$$label = B(F(E(p^{RGB}), E(p^{Depth}))), \tag{3}$$

where the p^{RGB}, p^{Depth} represent the RGB image and depth image, respectively. E represents the feature extraction module. F represents the feature fusion module, and B represents the binary classification module.

IV. EXPERIMENTS

In this section, we evaluate our method on the dataset generated from the public dataset KITTI [31]; we detail the data preprocessing, evaluation metrics, and training procedure and discuss the results of experiments.

A. Dataset preparation

We use the KITTI odometry branch to evaluate our proposed method. KITTI Odometry dataset consists of 21 sequences of different scenarios. The dataset provides calibration parameters between each sensor, and the calibration parameters between LiDAR and camera were obtained by [33], which are treated as the ground truth of extrinsic calibration parameters. This paper only considers the calibration self-check between the LiDAR and the left color camera. Specifically, we use sequences from 01 to 20 for train and validation (39011 frames) and sequence 00 for the test (4541 frames). The test dataset is spatially independent of the training dataset, except for a minimal subset sequence (about 200 frames), so it can be assumed that the test set is not in the training data.

TABLE I: Four configurations for the performance evaluation of the proposed network.

	positive		negative	
	roll=pitch=yaw	x=y=z	roll/pitch/yaw	x/y/z
configuration1	(-1,1)	(-0.1,0.1)	(-2,-1)∪(1,2)	(-0.2,-0.1)∪(0.1,0.2)
configuration2	(-1,1)	(-0.1,0.1)	(-5,-1)∪(1,5)	(-0.5,-0.1)∪(0.1,0.5)
configuration3	(-1,1)	(-0.1,0.1)	(-10,-1)∪(1,10)	(-1,-0.1)∪(0.1,1)
configuration4	(-1,1)	(-0.1,0.1)	(-20,-1)∪(1,20)	(-1.5,-0.1)∪(0.1,1.5)

B. Evaluation Metrics

As a classification task, we adopt the $accuracy$, $precision$, and $recall$ to show the ability of the proposed network. In binary classification tasks, there are four conditions in the final results: true positive (TP), true negative (TN), false positive (FP), and false negative (FN). Accuracy, precision and recall can be expressed in equations (4)-(6), respectively. $Accuracy$ represents the overall performance of the classifier. $Precision$ measures the severity of classifier misjudgment, and $recall$ measures how many samples are left out.

$$accuracy = \frac{TP + TN}{TP + TN + FP + FN} \tag{4}$$

$$precision = \frac{TP}{TP + FP} \tag{5}$$

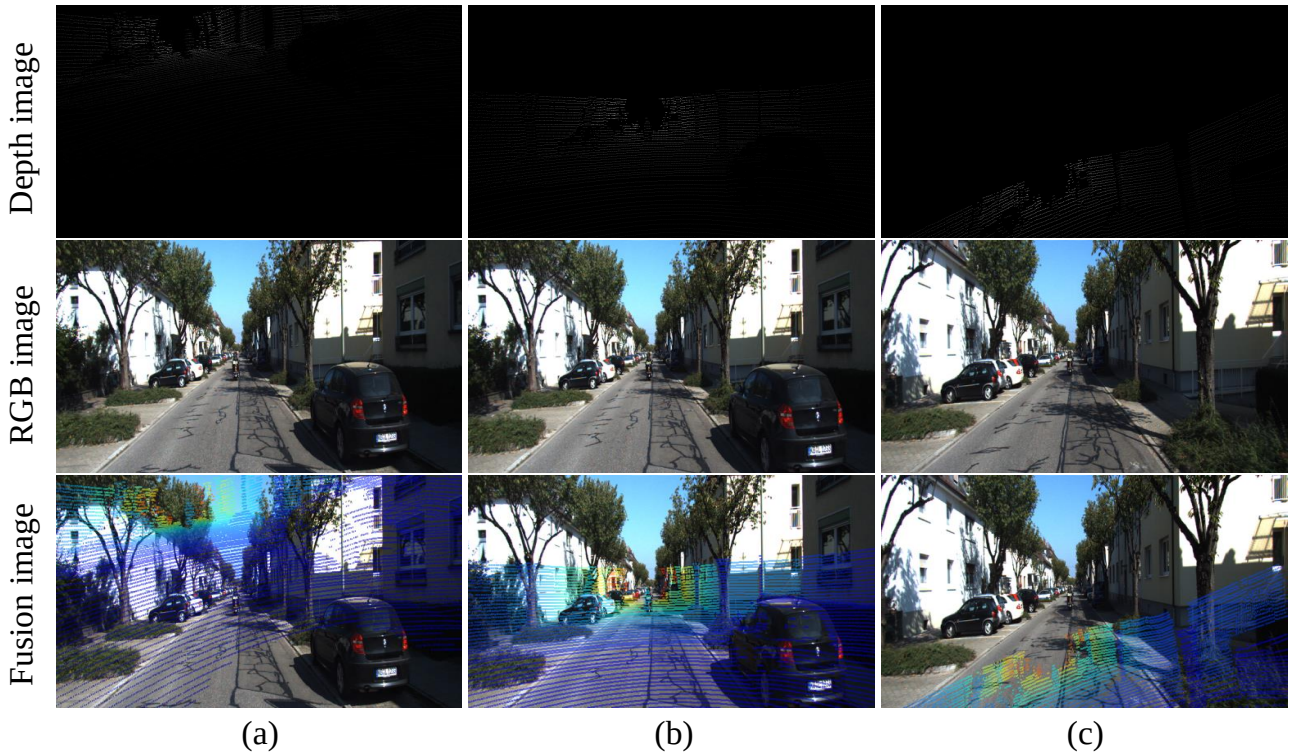

Fig. 3: The performance of LiDAR-camera calibration self-check.

$$recall = \frac{TP}{TP + FN} \tag{6}$$

C. Training Details

In the training process, we use the Adam Optimizer with an initial learning rate of $3e^{-4}$. We train the proposed calibration self-check network on an NVIDIA 1080Ti GPU with a batch size of 48, and we train our model for 20 epochs. It is essential to note that we apply different disturbance ranges to transformations. As in equation (2), our disturbance only influences the extrinsic parameters. The disturbance range can be determined according to the tolerance of the downstream algorithm to the calibrated parameters. In order to test comprehensive performance, we prepare four different transformations for each point cloud. The configuration is illustrated in Tab I. In the four configurations, the positive samples have the same restriction that $roll, pitch, yaw$ disturbance starts from $-1°$ to $1°$ and x, y, z disturbance starts from $-0.1m$ to $0.1m$. However, the negative samples have different restrictions under different configurations. For example, in configuration1, at least one of $roll, pitch, yaw$ or x, y, z is in $(-2, -1) \cup (1, 2)$ or $(-0.2, -0.1) \cup (0.1, 0.2)$. The disturbance can be applied to point clouds by equation (2). the numbers of positive and negative samples are equal under each configuration listed in Tab. I. In practice, we load the pre-trained feature extraction layers from other tasks, and only fully connected layers are trained from scratch. Because of the numerous data in KITTI and the appropriate learning strategy, our network can converge quickly.

TABLE II: Experiments results

	configuration1	configuration2	configuration3	configuration4
accuracy	91.46	94.91	97.05	97.56
precision	88.20	91.80	94.93	95.94
positive recall	95.73	98.48	99.38	99.34

TABLE III: Inference time

	total samples	total times(s)	one sample(s)
configuration1	4541	384	0.08456
configuration2	4541	379	0.08346
configuration3	4541	380	0.08368
configuration4	4541	380	0.08368
average	4541	380.75	0.08385

D. Results and discussion

We test our method on sequence 00 of KITTI. The result is shown in Tab. II. In terms of accuracy, we get the highest score, 97.56% under configuration4. In terms of precision, we get the highest score, 95.94% under configuration4. In terms of recall, we get the highest score, 99.38%, under configuration3. Overall, in configuration1, the positive and negative data are much more similar; meanwhile, in configuration4, the gap between positive and negative data is relatively much larger. We also test the Inference time of our method, and the result is shown in Tab. **??**. The average inference time of one sample is $0.08385s$. The algorithm is

so fast and can be applied in real time. It shows excellent performance in LiDAR-camera calibration self-check. Some performance of our method is shown in Fig. 3. The rows of Fig. 3 represent depth, RGB, and Fusion images. The Fig. 3(a)(c) are negative data and the Fig. 3(b) is a positive data.

V. CONCLUSIONS

In this paper, We design an end-to-end LiDAR and camera calibration self-checking network, which exploit the feature extraction module, the feature fusion module and the binary classification layer to express the correlation between the RGB image and the depth image projected from point clouds. Our experiments on the proposed dataset branch demonstrate the performance of our method. This is the first work to address the significance of continually checking the calibrated extrinsic parameters for autonomous driving

REFERENCES

[1] A. Dosovitskiy, G. Ros, F. Codevilla, A. Lopez, and V. Koltun, "CARLA: An open urban driving simulator," in *Proceedings of the 1st Annual Conference on Robot Learning*, 2017, pp. 1–16.

[2] N. Schneider, F. Piewak, C. Stiller, and U. Franke, "Regnet: Multimodal sensor registration using deep neural networks," *CoRR*, vol. abs/1707.03167, 2017. [Online]. Available: http://arxiv.org/abs/1707.03167

[3] G. Iyer, R. K. Ram, J. K. Murthy, and K. M. Krishna, "Calibnet: Geometrically supervised extrinsic calibration using 3d spatial transformer networks," *2018 IEEE/RSJ International Conference on Intelligent Robots and Systems (IROS)*, Oct 2018. [Online]. Available: http://dx.doi.org/10.1109/IROS.2018.8593693

[4] K. Yuan, Z. Guo, and Z. J. Wang, "Rggnet: Tolerance aware lidar-camera online calibration with geometric deep learning and generative model," *IEEE Robotics and Automation Letters*, vol. 5, no. 4, pp. 6956–6963, 2020.

[5] C.-K. Chang, J. Zhao, and L. Itti, "Deepvp: Deep learning for vanishing point detection on 1 million street view images," in *2018 IEEE International Conference on Robotics and Automation (ICRA)*, 2018, pp. 4496–4503.

[6] Z. Teed and J. Deng, "Deepv2d: Video to depth with differentiable structure from motion," 2020.

[7] B. Ummenhofer, H. Zhou, J. Uhrig, N. Mayer, E. Ilg, A. Dosovitskiy, and T. Brox, "Demon: Depth and motion network for learning monocular stereo," *2017 IEEE Conference on Computer Vision and Pattern Recognition (CVPR)*, Jul 2017. [Online]. Available: http://dx.doi.org/10.1109/CVPR.2017.596

[8] Z. Yin and J. Shi, "Geonet: Unsupervised learning of dense depth, optical flow and camera pose," *CoRR*, vol. abs/1803.02276, 2018. [Online]. Available: http://arxiv.org/abs/1803.02276

[9] Y. Zhou, Y. He, H. Zhu, C. Wang, H. Li, and Q. Jiang, "Monocular 3d object detection: An extrinsic parameter free approach," *CoRR*, vol. abs/2106.15796, 2021. [Online]. Available: https://arxiv.org/abs/2106.15796

[10] T. Zhou, M. Brown, N. Snavely, and D. G. Lowe, "Unsupervised learning of depth and ego-motion from video," 2017.

[11] O. Bogdan, V. Eckstein, F. Rameau, and J.-C. Bazin, "Deepcalib: A deep learning approach for automatic intrinsic calibration of wide field-of-view cameras," in *Proceedings of the 15th ACM SIGGRAPH European Conference on Visual Media Production*, ser. CVMP '18. New York, NY, USA: Association for Computing Machinery, 2018. [Online]. Available: https://doi.org/10.1145/3278471.3278479

[12] A. Kendall, M. Grimes, and R. Cipolla, "Posenet: A convolutional network for real-time 6-dof camera relocalization," 2016.

[13] J. Levinson and S. Thrun, "Automatic online calibration of cameras and lasers." in *Robotics: Science and Systems*, vol. 2, 2013, p. 7.

[14] G. Pandey, J. R. McBride, S. Savarese, and R. M. Eustice, "Automatic targetless extrinsic calibration of a 3d lidar and camera by maximizing mutual information." in *AAAI*, 2012.

[15] Y. Zhu, C. Li, and Y. Zhang, "Online camera-lidar calibration with sensor semantic information," in *2020 IEEE International Conference on Robotics and Automation (ICRA)*, 2020, pp. 4970–4976.

[16] W. Wang, S. Nobuhara, R. Nakamura, and K. Sakurada, "Soic: Semantic online initialization and calibration for lidar and camera," *arXiv preprint arXiv:2003.04260*, 2020.

[17] T. Ma, Z. Liu, G. Yan, and Y. Li, "Crlf: Automatic calibration and refinement based on line feature for lidar and camera in road scenes," 2021.

[18] G. Yan, F. He, C. Shi, X. Cai, and Y. Li, "Joint camera intrinsic and lidar-camera extrinsic calibration," 2022.

[19] J. Serafin and G. Grisetti, "Nicp: Dense normal based point cloud registration," in *2015 IEEE/RSJ International Conference on Intelligent Robots and Systems (IROS)*. IEEE, 2015, pp. 742–749.

[20] S. Rusinkiewicz and M. Levoy, "Efficient variants of the icp algorithm," in *Proceedings third international conference on 3-D digital imaging and modeling*. IEEE, 2001, pp. 145–152.

[21] J. Serafin and G. Grisetti, "Using augmented measurements to improve the convergence of icp," in *International Conference on Simulation, Modeling, and Programming for Autonomous Robots*. Springer, 2014, pp. 566–577.

[22] M. Magnusson, "The three-dimensional normal-distributions transform: an efficient representation for registration, surface analysis, and loop detection," Ph.D. dissertation, Örebro universitet, 2009.

[23] H. Deng, T. Birdal, and S. Ilic, "Ppfnet: Global context aware local features for robust 3d point matching," in *Proceedings of the IEEE conference on computer vision and pattern recognition*, 2018, pp. 195–205.

[24] Z. J. Yew and G. H. Lee, "Rpm-net: Robust point matching using learned features," in *Proceedings of the IEEE/CVF conference on computer vision and pattern recognition*, 2020, pp. 11 824–11 833.

[25] Z. Qin, H. Yu, C. Wang, Y. Guo, Y. Peng, and K. Xu, "Geometric transformer for fast and robust point cloud registration," in *Proceedings of the IEEE/CVF Conference on Computer Vision and Pattern Recognition*, 2022, pp. 11 143–11 152.

[26] P. Wei, G. Yan, Y. Li, K. Fang, W. Liu, X. Cai, and J. Yang, "Croon: Automatic multi-lidar calibration and refinement method in road scene," 2022.

[27] X. Lv, B. Wang, Z. Dou, D. Ye, and S. Wang, "Lccnet: Lidar and camera self-calibration using cost volume network," in *Proceedings of the IEEE/CVF Conference on Computer Vision and Pattern Recognition*, 2021, pp. 2894–2901.

[28] J. Shi, Z. Zhu, J. Zhang, R. Liu, Z. Wang, S. Chen, and H. Liu, "Calibrcnn: Calibrating camera and lidar by recurrent convolutional neural network and geometric constraints," in *2020 IEEE/RSJ International Conference on Intelligent Robots and Systems (IROS)*. IEEE, 2020, pp. 10 197–10 202.

[29] X. Lv, S. Wang, and D. Ye, "Cfnet: Lidar-camera registration using calibration flow network," *Sensors*, vol. 21, no. 23, p. 8112, 2021.

[30] A. Geiger, P. Lenz, C. Stiller, and R. Urtasun, "Vision meets robotics: The kitti dataset," *The International Journal of Robotics Research*, vol. 32, no. 11, pp. 1231–1237, 2013.

[31] A. Geiger, P. Lenz, and R. Urtasun, "Are we ready for autonomous driving? the kitti vision benchmark suite," in *2012 IEEE conference on computer vision and pattern recognition*. IEEE, 2012, pp. 3354–3361.

[32] D. Sun, X. Yang, M.-Y. Liu, and J. Kautz, "Pwc-net: Cnns for optical flow using pyramid, warping, and cost volume," in *Proceedings of the IEEE conference on computer vision and pattern recognition*, 2018, pp. 8934–8943.

[33] A. Geiger, F. Moosmann, Ö. Car, and B. Schuster, "Automatic camera and range sensor calibration using a single shot," in *2012 IEEE international conference on robotics and automation*. IEEE, 2012, pp. 3936–3943.

[34] P. C. Ng and S. Henikoff, "Sift: Predicting amino acid changes that affect protein function," *Nucleic acids research*, vol. 31, no. 13, pp. 3812–3814, 2003.

[35] H. Bay, T. Tuytelaars, and L. V. Gool, "Surf: Speeded up robust features," in *European conference on computer vision*. Springer, 2006, pp. 404–417.

[36] N. Schneider, F. Piewak, C. Stiller, and U. Franke, "Regnet: Multimodal sensor registration using deep neural networks," in *2017 IEEE intelligent vehicles symposium (IV)*. IEEE, 2017, pp. 1803–1810.

[37] G. Iyer, R. K. Ram, J. K. Murthy, and K. M. Krishna, "Calibnet: Geometrically supervised extrinsic calibration using 3d spatial transformer

networks," in *2018 IEEE/RSJ International Conference on Intelligent Robots and Systems (IROS)*. IEEE, 2018, pp. 1110–1117.

[38] Z. Li, X. Wang, X. Liu, and J. Jiang, "Binsformer: Revisiting adaptive bins for monocular depth estimation," *arXiv preprint arXiv:2204.00987*, 2022.

[39] W. Yuan, X. Gu, Z. Dai, S. Zhu, and P. Tan, "New crfs: Neural window fully-connected crfs for monocular depth estimation," *arXiv preprint arXiv:2203.01502*, 2022.

[40] W. Zheng, W. Tang, L. Jiang, and C.-W. Fu, "Se-ssd: Self-ensembling single-stage object detector from point cloud," in *Proceedings of the IEEE/CVF Conference on Computer Vision and Pattern Recognition*, 2021, pp. 14 494–14 503.

[41] Q. Xu, Y. Zhou, W. Wang, C. R. Qi, and D. Anguelov, "Spg: Unsupervised domain adaptation for 3d object detection via semantic point generation," in *Proceedings of the IEEE/CVF International Conference on Computer Vision*, 2021, pp. 15 446–15 456.

[42] K. He, X. Zhang, S. Ren, and J. Sun, "Deep residual learning for image recognition," in *Proceedings of the IEEE conference on computer vision and pattern recognition*, 2016, pp. 770–778.

[43] A. L. Maas, A. Y. Hannun, A. Y. Ng, *et al.*, "Rectifier nonlinearities improve neural network acoustic models," in *Proc. icml*, vol. 30, no. 1. Citeseer, 2013, p. 3.